Alignment and Relaxation Dynamics of Dye Molecules in Host−Guest Inclusion Compounds As Probed by Dielectric Spectroscopy

Julius Tsuwi,[†] Ricarda Berger,[†] Gaël Labat,[†] Gaëtan Couderc,[†] Norwid-Rasmus Behrnd,[†] Phillipp Ottiger,[†] Fabio Cucinotta,[‡] Klaus Schürmann,[‡] Mariana Bertoni,[¶,§] Lucas Viani,[||] Johannes Gierschner,[#,||] Jérôme Cornil,[||] Anna Prodi-Schwab,[§] Luisa De Cola,[‡] Michael Wübbenhorst,[⊥] and Jürg Hulliger*[,†]

Department of Chemistry and Biochemistry, University of Berne, Freiestrasse 3, CH-3012 Berne, Switzerland, Physikalisches Institut, Westfälische Wilhelms-Universität Münster, Mendelstrasse 7, D-48149 Münster, Germany, Evonik Degussa GmbH, Creavis Technologies and Innovation, Paul-Baumann-Strasse 1, D-45772 Marl, Germany, Laboratory for Chemistry of Novel Materials, University of Mons, Place du Parc 20, B-7000 Mons, Belgium, and Laboratory for Acoustics and Thermal Physics, Department of Physics and Astronomy, Katholieke Universiteit Leuven, Celestijnenlaan 200D, B-3001 Heverlee, Belgium

Received: March 18, 2010; Revised Manuscript Received: May 14, 2010

The alignment and relaxation dynamics of a polar dye molecule, *N*,*N*-dimethyl-4(4-nitrophenylazo)aniline (DNAA), in zeolite L and perhydrotriphenylene (PHTP) channels were investigated by means of a combination of optical, dielectric, and quantum-chemical methods. Both the zeolite L and PHTP channels enable the dye molecules to align along the channel axis. An amplified net dipole moment of DNAA in PHTP is observed and attributed to enhanced 1D close alignment of dye molecules. In zeolite L channels, a concentration gradient is found with aggregation at the channel entrances. The dynamics of the dye in zeolite L channels reveals localized conical rotational fluctuation modes following Arrhenius-type activation with energy of 0.31 eV, which we assign to small noninteracting fluctuating polar units of the dyes being loosely aligned or isolated. Unlike zeolite L, relaxations in PHTP are characterized by cooperative wobbling motions interpreted as increased intermolecular dipole interaction due to a closely packed one-dimensional array. Temperature-dependent activation energies of 0.25 eV below 0 °C and 0.37 eV at ambient temperature reflect the role of the soft channel walls in the activation process.

1. Introduction

Organic chromophores, such as *N*,*N*-dimethyl-4(4-nitrophenylazo)aniline (DNAA)(Figure 1), have attracted much attention as active compounds in optoelectronic applications. Understanding the fate of optically excited states or the transport of photonic excitations (or charges) is of importance in optimizing the properties of such devices. Their applications on the market "real life" is, however, impeded by aggregation effects[1,2] and photostability.[3,4] Such problems can be overcome by confining the chromophores into channel-forming host materials such as zeolite L[5−7] or perhydrotriphenylene (PHTP)[8−17] (see Figure 1). The mobility of guest molecules in the channels is of significance for high-precision calculations of excitation energy transfer in light harvesting devices[18,19] as well as in the design of functional architectures that require a certain extent of molecular mobility, such as molecular switches.

In the channels, however, it is expected that the mobility of the DNAA guest is significantly restricted as compared with

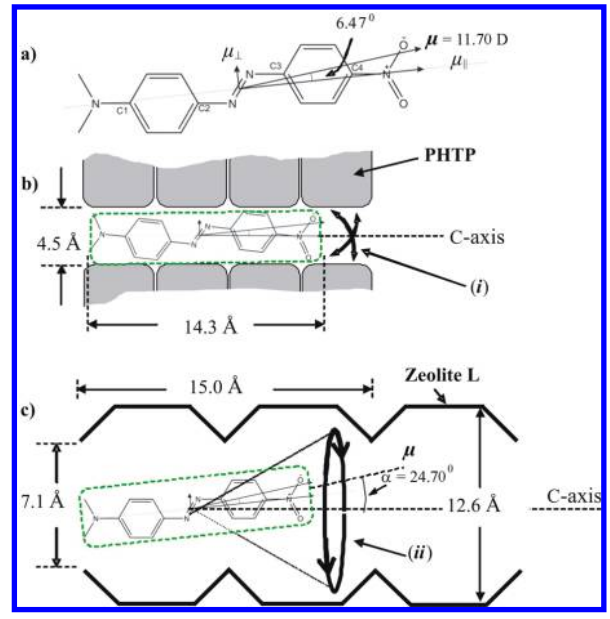

Figure 1. (a) Chemical structure of *N*,*N*-dimethyl-4(4-nitrophenylazo)aniline (DNAA) molecule used in the study. Molecular dipole moment $\boldsymbol{\mu} = 11.17$ D is shown following convention that direction is toward negative charge. The dipole components $\mu_\perp = 1.25$ D and $\mu_\parallel = 11.10$ D are taken about the molecular center of mass. The illustration of (b) DNAA/PHTP and (c) DNAA/zeolite L inclusion compounds are also shown with view perpendicular to the crystal *c*-axis. Dynamics of DNAA in the channels is characterized by cooperative wobbling motion (*i*) in PHTP and conical local fluctuation (*ii*) in zeolite L.

* Corresponding author. Phone: +41 31 631 4242. Fax: +41 31 631 4244. E-mail: publication.hulliger@iac.unibe.ch.
[†] University of Berne.
[‡] Westfälische Wilhelms-Universität Münster.
[§] Evonik Degussa GmbH.
[||] University of Mons.
[⊥] Katholieke Universiteit Leuven.
[¶] Current address: Department of Mechanical Engineering, Massachusetts Institute of Technology, Cambridge, MA 02139.
[#] Madrid Institute of Advanced Studies (IMDEA-Nanoscience) UAM, Module C-IX, Third Level, Av. Tómas y Valiente 7, Campus Cantoblanco, E-28049 Madrid, Spain.

10.1021/jp102451w
Published on Web 06/10/2010

the crystalline form. The possible degrees of freedom of guest molecules in a channel matrix comprise both intra- and intermolecular motions, depending on the rigidity of the channel environment.[20] For PHTP, previous studies by solid-state ^{13}C and ^{2}H NMR,[21,22] fluorescence excitation,[22] and Raman spectroscopy[23] as well as by quantum-chemical[20,23,24] and molecular dynamics calculations[20,25] on nonpolar saturated[21] and unsaturated[20,23] hydrocarbon guests, have revealed the tight but soft nature of the surrounding PHTP host environment and its impact on the guest dynamics. For polar guest inclusions, additional relaxation modes are expected which result from the guest polarity. These modes are not expected to be captured by the techniques mentioned above. Thus, by employing the dielectric technique in this study, we have the advantage to monitor additional mobility by probing relaxation modes of the guest polar groups. Being polar, DNAA represents a prototype molecule for probing the effect of the matrix on the guest mobility in inclusion compounds.

The two channel-forming host systems, the inorganic zeolite L and the organic PHTP, differ in many respects. On one hand, the PHTP-based molecular cocrystal sets up a tightly packed but rather soft environment for rod-shaped molecules (see Figure 1) to form an almost perfect unipolar 1D collinear alignment[8,10] adopting transversal motion only by lattice dynamics.[22] The inorganic frame, on the other hand, is more rigid, more cavity-like, and features ionic charges;[26−28] thus, neither 1D close packed loading nor full collinear alignment is possible here. Unipolarity of dipole alignment is governed by orientational selectivity at the interface of channel entrances.[29]

In this paper, we report the dynamics of a polar DNAA probe in the confinement of zeolite L and PHTP channel environments. We use dielectric relaxation spectroscopy (DRS) to reveal information about molecular dynamics of guest species, thus allowing us to obtain a detailed picture on the mobility of a nanometer-sized guest molecule inside the nanochannels. DRS has the advantage, by utilizing a broad frequency and temperature range, to distinguish between intramolecular motions such as localized dipole fluctuations as well as overall intermolecular reorientations of the molecule within its environment. The combined polarized optical and dielectric methods together with quantum-chemical calculations reveal the alignment and close packing state of the guest molecule in both channel confinements; hence, providing a deeper understanding of molecular mobility in confined spaces.

2. Experimental

2.1. Synthesis and Dye Loading in Channels. Racemic PHTP was synthesized as described in ref 30, and zeolite L, as reported in refs 31 and 32. The *N*,*N*-dimethyl-4-(4-nitrophenylazo)aniline (DNAA) guest molecule (dye) was prepared according to refs 33 and 34. Due to the nature of the channels in both hosts, the inclusion compounds were prepared in two different ways. For the purpose of ion exchange, the zeolite L was stirred in an aqueous solution of KNO_3 (1 mol/L, 5 h, 50 °C). Separated crystals were washed with double-distilled water and centrifuged until neutral pH and then dried at 70 °C overnight. The loading of the dye followed a well-established gas-phase insertion procedure[27] at 175 °C. To remove dye molecules adsorbed on the outer surface, the zeolite L crystals were rinsed repeatedly with a 1:500 Genapol X-080 (Fluka)-to-water solution until fluorescence was not detected in the washing solutions. The loading fraction (p) of the dye in the channels was estimated to be 0.32 (see the Supporting Information for the determination of dye loading). The organic PHTP inclusion compound was prepared by slow cooling cocrystallization from bromoform.[35]

2.2. Sample Preparation and Characterization. ***2.2.1. Polarization Microscopy.*** To prepare thin crystals appropriate for optical measurements, a droplet of DNAA/PHTP dissolved in bromoform was deposited on a microscope slide for evaporation at room temperature. Well-developed crystals were dispersed in ethanol and analyzed with a Leitz microscope DM RXP (built-in polarizers, coupled to a Sony XC-950 P CCD camera). The samples were irradiated with linear polarized light in transmission mode, and pictures were taken in real color.

2.2.2. Fluorescence and Confocal Microscopy. Zeolite L crystals of type NZL 40 (Clariant) of diameter 1 mm and an average length of 3.5 mm were used for the experiments. Fluorescence microscopy was carried out with an Olympus BX-41 equipped with a Hg high-pressure lamp; MBFL3, MWU2, U-MWB2, and U-MWG2 excitation cubes (bright field, UV, blue and green, respectively); an air objective 100 × 1.0; a color camera; and a polarizer. Confocal microscopy and lifetime distribution measurements were carried out on a PicoQuant Microtime 200 time-resolved confocal microscope with a laser diode (excitation at 400 nm, repetition frequency 40 MHz) and 100 × (NA 1.4) oil immersion objective. The emission was detected using two single photon avalanche diodes set after a 460 nm long pass filter. The spectra of single crystals were recorded on a fiber coupled spectrograph (Andor-Shamrock 163) and EMCCD camera (Andor Newton DU970N) upon excitation at 375 nm.

2.2.3. Dielectric Relaxation Experiments. For dielectric relaxation measurements, the materials were pressed into pellets of 10 mm diameter and a thickness in the range 0.6−1.3 mm (kept between two brass electrodes). To improve the electrical contact with the plate electrodes, the pellets were coated with a thin layer of silver paste. Isothermal dielectric measurements were performed in the frequency range of $1-10^7$ Hz using a high-resolution dielectric Alpha-analyzer (Novocontrol GmbH). Generally, to erase any thermal history, samples were first heated from room temperature to 100 °C and kept at this temperature for 30 min. For zeolite L samples, a more elaborate annealing procedure to eliminate adsorbed water[36−39] was carried out for which the samples were kept at 120 °C for 17 h before measuring. The dielectric spectra were then obtained starting from high temperature down to −120 °C and then back to high temperatures in intervals of 2 °C. The high temperature limit was chosen carefully taking into consideration the melting temperatures of the different samples. The sample temperature was controlled by a gas heating system based on evaporation of liquid nitrogen (Quatro, Novocontrol GmbH) with a precision of ±0.2 °C. Details of the setup are found elsewhere.[40]

To analyze the data, the dielectric loss ε'' was fitted to a superposition of a conductivity contribution with one or two relaxation functions according to the empirical formula (eq 1) by Havriliak and Negami (HAVNEG).[41]

$$\varepsilon''(\omega) = \frac{\sigma_o}{\varepsilon_o}\frac{a}{\omega^s} + \mathrm{Im}\{\Delta\varepsilon/[1 + (i\omega\tau)^\kappa]^\lambda\} \qquad (1)$$

The first term on the right-hand side of the equation describes the conductivity, whereas the second one corresponds to the dipole contribution to the dielectric loss function. In this notation, just one relaxation process is assumed. κ and λ are dimensionless parameters describing the symmetric and asymmetric broadening of the distribution of relaxation times,

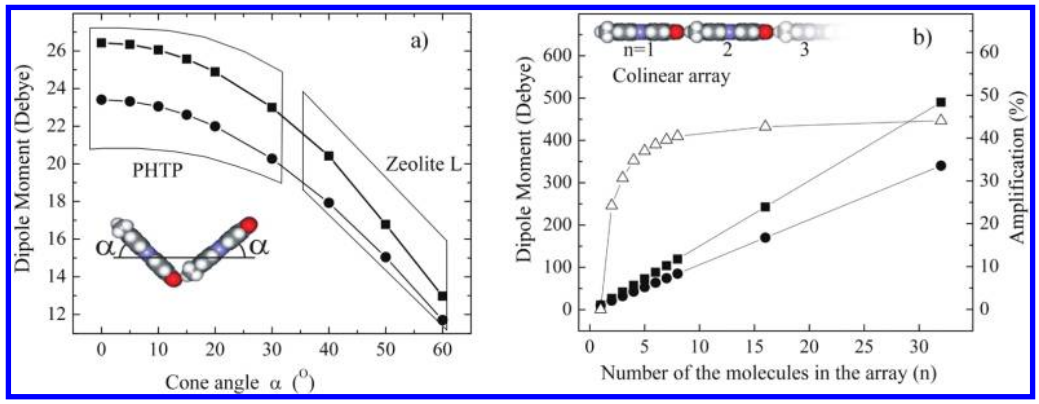

Figure 2. (a) Evolution of the net dipole moment in a head-to-tail dimer (■) and in a dimer made of two isolated (•) DNAA molecules in channels as a function of the cone angle α, as obtained from DFT calculations; (b) calculated total parallel dipole moment ($\mu_{\parallel}$) of a head-to-tail 1D array and of the corresponding isolated molecules. The percentage of dipole amplification (△) as a result of the head-to-tail (angle α = 0) arrangement vis-à-vis isolated dipole arrangement is seen to reach a plateau of 45% at ∼32 molecules.

respectively, with $0 < (\kappa, \kappa\lambda) \leq 1$. For $\kappa = \lambda = 1$, eq 1 simplifies to the ideal Debye[42] relaxation. ε_o is the permittivity of free space, and σ_o is the direct current (dc) conductivity. The exponent s equals 1 for ohmic behavior, and deviations ($s < 1$) are a result of electrode polarization or Maxwell−Wagner polarization effects (a is a factor having the dimensions $[\mathrm{Hz}]^{s-1}$, for $s \neq 1$). From the fits according to eq 1, the relaxation rate $1/\tau_{max}$ can be deduced, which is given at the frequency of maximum dielectric loss ε'' at a fixed temperature, T. Within experimental uncertainty, eq 1 describes our data well. The term $\Delta\varepsilon$ is the dielectric strength, which can be used to estimate the value of the net dipole moment taking part in the relaxation process. This can be done through the Kirkwood−Fröhlich theory from the relation[43−46]

$$\Delta\varepsilon \approx \rho_{\mu}\frac{\mu^2}{3k_{\mathrm{B}}\mathrm{T}\varepsilon_o}g \qquad (2)$$

where g represents the Kirkwood−Fröhlich dipole correlation factor, μ is the net dipole moment, ρ_{μ} is the dipole density, k_{B} is the Boltzmann constant, and T is the absolute temperature.

2.2.4. Quantum-Chemical Calculations of Dipole Enhancement in a Chain. All calculations were done at the density functional theory (DFT) level (employing the B3LYP functional[47] and 6-31+G* basis set within the Gaussian03 program package[48]). The evolution of the net dipole moment for a head-to-tail arrangement of a 1D array of DNAA molecules was calculated by varying the angle α (see Figure 2) with respect to alignment along the channel axis. The intermolecular separation was fixed to 16.84 Å between centers of mass, which corresponds to the interguest van der Waals distance for a perfect head-to-tail alignment.

3. Results and Discussion

3.1. DNAA: Electric Dipole Moment and Static Orientation in Channels. Figure 1a shows the projection of the DFT calculated net dipole moment ($\mu = 11.70$ D) of a single DNAA molecule in free space in the molecular plane with its smaller transversal ($\mu_{\perp} = 1.32$ D) and larger longitudinal ($\mu_{\parallel} = 11.63$ D) components. If the main molecular axis is defined in the direction between the N of the nitro group and the N of the amino group, the orientation of the net dipole moment deviates by an angle of 6.47° from this main axis. The components of the dipole reflect the molecule's symmetry m (or C_s) and trans configuration.[33] The experimental net dipole moment of a DNAA molecule is reported in the literature to be 7.5 ± 0.7 D;[49−51] differences between experimental and calculated values are attributed to solvent effects.[51] DNAA forms antiparallel polar chains (acentric point group 2) that minimize the alignment of dipoles by orientational disorder of the azo moiety.[33] The 25% probability of orientational disorder in the inversion of the −N═N−azo moiety reported in ref 33 results in the reduction of the effective transversal ($\mu_{\perp}$) dipole component by the same amount.

In the channels of zeolite L or PHTP, antiparallel chain stacking within one channel is prohibited, and thus, single molecules align themselves along the channel as depicted in Figure 1b for DNAA in PHTP and Figure 1c for zeolite L channels. Zeolite L has an entrance width of 7.1 Å, and PHTP is somewhat capable of adapting its channel width with respect to the guest, which for the case of DNAA, is 4.5 Å. Thus, due to spatial restrictions,[5−17] no side-by-side stacking of DNAA molecules in the same channel is expected.

It has been argued in literature that the static arrangement of guest molecules is governed by a head-to-tail arrangement in zeolite L[5−7] and PHTP[8−17] channels. Dipole orientation is thus similar, such that associated relaxations are confined to accessible angles α. Qualitatively, Figure 1 shows that an isolated DNAA molecule can assume a larger α angular distribution in zeolite L than in PHTP channels. In zeolite L, by assuming a center of mass of DNAA around the −N═N− bonds, the terminal groups [NO_2 or $N(CH_3)_2$] can sweep through a transversal distance of ∼3.28 Å with respect to the c-axis. Given that DNAA occupies two cells when inserted in zeolite L with internal cross section diameter of 12.66 Å, it is evident that the transversal sweep can be enhanced 3-fold at elevated thermal agitation. In other words, larger angles α can be attained in zeolite L than in PHTP. This is shown quantitatively in Figure 2a, where the evolution of μ as calculated by DFT is plotted as a function of the cone angle α in a head-to-tail DNAA dimer as compared with a dimer made of two isolated molecules in both channels.

The fluctuation angle, α, is estimated (in first approximation) from geometric factors: namely, the length of the DNAA molecule and the space provided by channels. For zeolite L, α was determined by Megelski et al[7] to have a maximum at 72° for oxonine molecule of 11.3 Å in length. Since DNAA is longer (14.3 Å), we shall assume here an angle α < 72°. In PHTP, the diameter of the channels is much smaller, and molecules feel no free space for large α values. However, PHTP walls are more dynamic, allowing enhanced α values by thermal agitation.[22,23]

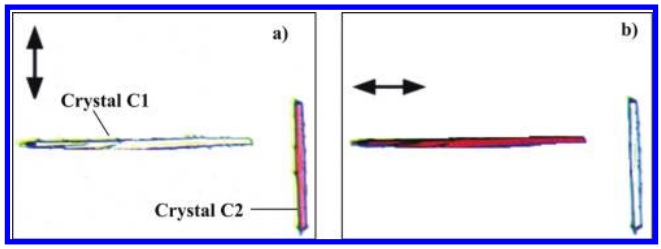

Figure 3. Dichroism of DNAA in PHTP with direction of polarized light (black double arrow) rotated by 90° to the direction of channel *c*-axis.

Consequently, these considerations indicate that large fluctuation angles α up to 60° are associated with zeolite L and low ones up to 30° to PHTP.

Calculations of the resulting $\mu_{||}$ dipole moment of a 1D molecular array of head-to-tail (collinear) oriented molecules (Figure 2b) show dipole higher by 45% (amplification) as compared with the sum of the dipole contributions of noninteracting molecules. This amplification of $\mu_{||}$, which is attributed to polarization-induced cooperative interactions,[52,53] saturates at about 10 molecules; that is, a chain length of 14.3 nm. Assuming 100% channel loading, the DNAA/PHTP crystal is expected to be *more polar* (because of the 45% dipole amplification) as compared with solid-state pristine DNAA crystal[54] due to the strongly enhanced global dipole moment resulting from the alignment of chains along the channel axes. For the case of the DNAA/zeolite L crystal, the global dipole moment is expected to be lower than that of DNAA/PHTP crystal owing to the larger range of accessible α angles that reduces the $\mu_{||}$ component. The enhanced polarity of the channels has a nontrivial impact on the molecular mobility as well as polarity-dependent properties such as optical anisotropy. Although the interaction between the dimethylamino and nitro groups is apparently weak, the dipole orientation and its subsequent amplification in the channels will lead to different relaxation mechanisms as compared with the pristine crystalline DNAA.[54]

3.2. DNAA Molecular Alignment and Distribution in Channels: Polarized Fluorescence and Confocal Microscopy. The preferential orientation of the DNAA molecules along the channel axis can be experimentally accessed by polarized absorption and fluorescence spectroscopic and microscopic techniques, as was done for other guest molecules in zeolite L[7,27] and PHTP.[10] Figure 3 shows two crystals of DNAA/PHTP of ∼3−5 mm in length under polarized light. The crystals are arranged perpendicular to each other. Upon illumination with polarized light parallel to the channel *c*-axis, a red color is observed (crystals C2 in a and C1 in b), but no red shows up for the crystal perpendicular to the polarized light. Although the dichroism observed by polarized microscopy is very significant, the *m* molecular symmetry does not imply a unique molecular axis. Therefore, a contribution from $\mu_{\perp}$ remains. However, we can assume that this contribution can cancel out by a two-dimensional (2D) rotational disorder.

For the micrometer-sized samples of zeolite L host−guest crystals, fluorescence experiments were preferred instead of polarized microscopy. Figure 4 shows fluorescence microscopy images of DNAA in zeolite L. Similar to the case of PHTP, both the crystals in *i* are visible when an unpolarized light source is used. Under polarized conditions, the DNAA/zeolite L system also shows a preferred general alignment (see Figure 4 *ii*, *iii*). It can be seen that the other two crystals perpendicular to the polarization direction are partially extinguished. It should be noted here that the preference to occupy specific sites in zeolite L [7,55] impedes the almost perfect alignment observed in PHTP. Thus, perpendicular components against the main crystal axis are partially visible, as also observed in other zeolite L loaded systems.[7,55,56]

To trace the spatial distribution of guests, we used a confocal microscopy. The crystal used in the experiment contains ∼2.65 × 10^{11} channels (number of channels = $0.265d^2$, where *d* is the channel diameter).[7,55,56] The loading fraction determined in Section 2.1 yields a 32% occupation probability[31,32] of DNAA molecules along each zeolite L channel. This translates in to roughly 783 000 guest molecules per channel out of the expected 2 448 000 for 100% filling. The fluorescence lifetime distribution as obtained from confocal microscopy (Figure 5) ranges from 1.5 to 2.5 ns. Slower excited state relaxations take place inside the channels while faster processes are localized close to the entrances, similar to previous observations in other dye-loaded zeolite L systems.[57] The inhomogeneous lifetime distribution indicates two different nanoenvironments of the dye molecules within the zeolite L channels. First, the middle part with its long lifetimes reflects a relatively sparse population with predominantly *monomeric* units. Second, toward the channel entrances, (partial) aggregation of dye molecules[57−59] are detected, reflected as shorter lifetimes and moderately red-shifted emissions due to exciton coupling between neighboring molecules. The aggregation might be a result of the loading process in which dyes stack at the entrances, pushing previous guests deeper into the channel, thus resulting in a concentration gradient.

All together, despite the similarities between the inorganic zeolite L and the organic host PHTP (of hexagonal symmetry with similar interchannel distances and channel diameters), pronounced differences exist. In zeolite L, the dyes are inhomogeneously distributed in rigid but somewhat spacious cavities, which lead to partial aggregation as well as to pronounced deviations from collinear arrangement along the channel axis. In the case of PHTP, the unipolar oriented dye molecules are homogenously distributed in a close-fitting but soft host environment. With this in mind, we will now see how such a density distribution and alignment influences the dynamics and, hence, the mobility of the molecules in both hosts by analyzing the dielectric relaxation data.

3.3. Relaxation of DNAA in Zeolite L and PHTP Channels: the γ and β_c Processes. Dielectric technique utilizes the application of an alternating electric signal to a material at a fixed frequency. When the material contains polar units, the dipoles tend to follow the polarization of the applied field. However, because of phase differences, the dielectric constant is a complex function $\varepsilon^*(\omega) = \varepsilon'(\omega) - i\varepsilon''(\omega)$, where $\varepsilon'(\omega)$ and $\varepsilon''(\omega)$ are the frequency dependent real and imaginary parts, respectively. The $\varepsilon''(\omega)$ function is proportional to the dielectric energy loss, that is, the dielectric loss, ε. When the characteristic relaxation time τ of a fluctuating dipole corresponds to that of an applied frequency ($f \propto 1/\tau$), the dielectric loss ε'' goes to a maximum, according to eq 1. Since ε'' is the effective average loss over all unique dipoles present in the molecule, the analysis of the dielectric loss as a function of frequency and temperature ε'' (ω, T) reveals important parameters such as the relaxation time of the polar units. The static molecular dipole moment μ has a *fixed* orientation with respect to the molecular geometry; thus, changes in μ can be directly associated with molecular motions, such as twists, turns, rotations, or flips of parts or the whole molecule, if the spatial restrictions of the environment allow them.

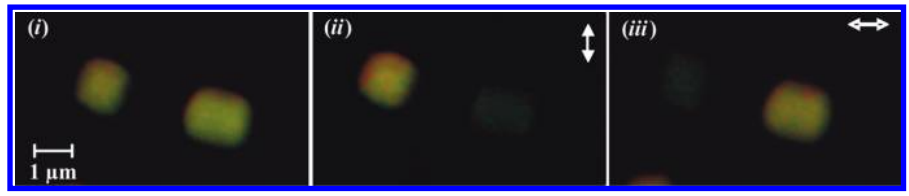

Figure 4. Fluorescence microscopy images of DNAA loaded zeolite L crystals showing polarization effects in *ii* and *iii*. The fluorescence picture in part *i* is taken from unpolarized light source for reference purposes. The direction of polarization is shown by the white double-arrow.

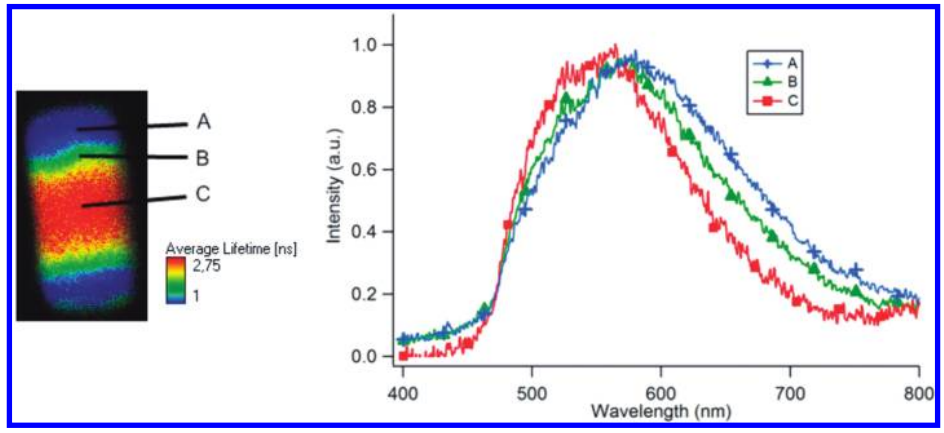

Figure 5. Confocal time- and space-resolved microscopy images of a single DNAA loaded zeolite L crystal showing the emission lifetime distribution (left) and the corresponding emission spectra (right). Letters A, B, and C correspond to three different zeolite L areas with an emission profile, indicating a moderate red-shift of the band when moving from the central part of the crystal to the ends, where the excitonic coupling is larger.

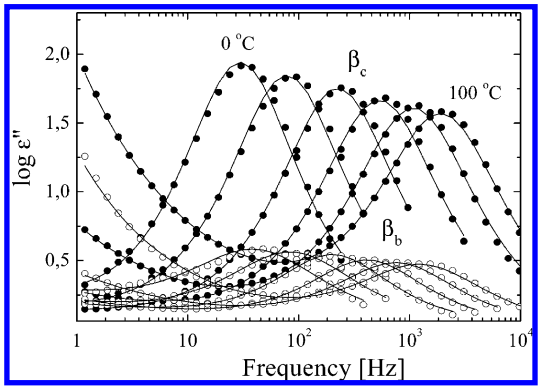

Figure 6. Dielectric loss, ε'', versus frequency for DNAA inside PHTP (filled circles) showing the β_c process. The data are compared with the solid state crystalline DNAA (open circles) data, taken from ref 54 at the same temperatures (0−100 °C in steps of 20 °C). The error bars are comparable to the size of the symbols, if not indicated otherwise.

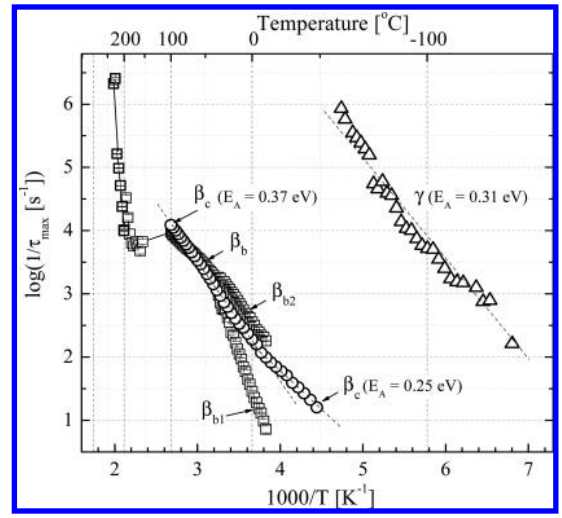

Figure 7. Temperature dependence of the relaxation times of DNAA inside zeolite L (△) and DNAA inside PHTP (○). The activation energies, E_A, of the relaxation processes in the different channels are indicated. The data is compared to solid state crystalline DNAA (□) data (relaxation processes β_b, β_{b1}, and β_{b2}) taken from ref 54.

Figure 6 shows the dielectric loss $\varepsilon''(\omega)$ for DNAA in PHTP channels in the temperature range of 0−100 °C together with data of solid state pristine DNAA crystal, taken from ref 54 for comparison. No relaxation peaks of DNAA in zeolite L channels could be found in this temperature range. The relaxation times τ (taken at peak maximum according to eq 1) are plotted against reciprocal temperature in Figure 7 for DNAA in channels and compared with the pristine DNAA data[54] and their corresponding dielectric strengths $\Delta\varepsilon$ depicted in Figure 8. In ref 54, details of the relaxation dynamics of pristine DNAA is described, being characterized by intramolecular fast local dipole fluctuations as well as intermolecular slow cooperative relaxation processes. In this work, the inclusion compounds of DNAA in zeolite L and PHTP channels show only a *single* relaxation process (γ and β_c, respectively) at all temperatures, as discussed below.

3.3.1. Relaxation in Zeolite L Channels. The γ process for DNAA/zeolite L is observed below −50 °C featuring a weak ε'' intensity and a dielectric strength ($\Delta\varepsilon$) below 0.1 over the entire range of temperature observed. The small $\Delta\varepsilon$ values reflect the low DNAA loading density of 32% in the sample (Section 2.1). Keeping in mind that DNAA occupies more than one cavity within the zeolite L framework[56,60] (Figure 1c), space confinement impedes relaxation by rotation around a *short* molecular axis. Large angular rotations, up to 60° as explained in Figure 2a, are possible only if the relaxation is by conical librations/rotations (around a long molecular axis) that are activated largely by the presence of the $\mu_\perp$ dipole component. From Figure 7, the γ relaxation exhibits Arrhenius-type temperature dependence,[61] described by the relation

$$1/\tau = 1/\tau_0 \exp(-E_A/RT) \qquad (3)$$

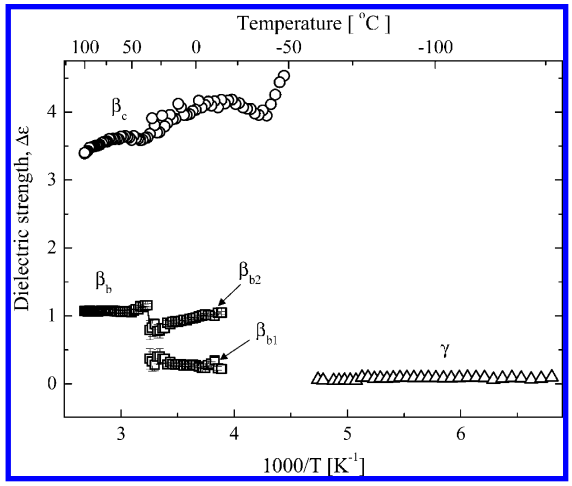

Figure 8. Temperature dependence of the dielectric strengths of DNAA inside zeolite L (△) and DNAA inside PHTP (○). The data is compared with solid state crystalline DNAA (□) data (relaxation processes β_b, β_{b1}, and β_{b2}) taken from ref 54.

where E_A is the activation energy, τ is the relaxation time, τ_0 is the limiting relaxation time at high temperature, R is the gas constant, and T is the absolute temperature. Given its Arrhenius thermal activation, the γ relaxation favors assignment to local molecular motions.[40,61] It is at least 5 orders of magnitude faster than the β_c process in PHTP as well as the processes found in the pristine DNAA[54] (Figure 7). The E_A of the γ process is 0.31 eV (∼30.4 kJ/mol), which is in a similar range to that found for pristine DNAA in ref 54. The limiting value[40] of $f_0 = 10^{13}$ Hz suggests that the surrounding host channel slightly hinders the γ relaxation, thus suggesting fluctuations of *isolated* molecules. Being isolated, DNAA molecules in the zeolite L channels have more torsional mobility around the N−Ci (i = 1, 2, 3 and 4) bonds (see Figure 1) than in the crystalline state, where mobility is quickly damped. Furthermore, the molecular dipole moment is optimized in the channel as compared with the crystalline state, where it is reduced to 75% due to the antiparallel crystal packing.[33,54] Thus, the dipole mobility is enhanced in the channels, which explains its observation at low temperatures. The activation energy barriers of the γ process matches that observed for pristine DNAA, which was attributed to the intramolecular rotational or torsional mobility.[54] No additional relaxation process is observed in zeolite L: no hints for molecular stacks or additional relaxation modes in the channels are deduced from the dielectric results. The aggregates at the zeolite L channel entrances as observed by confocal time- and space-resolved microscopy data do not result in any detectable unique (collective) dielectric relaxation. This points to disordered arrangements in the aggregates (rather than to ordered stacks) that still maintain their single molecule dipolar relaxation behavior.

3.3.2. Relaxation in PHTP Channels. From Figure 6, two features of the temperature dependence of the dielectric loss ε'' are noticeable. First, the intensity of ε'' and the dielectric strength $\Delta\varepsilon$ (see Figure 8) for the β_c process in the DNAA/PHTP system are at least three times higher than for the β_b process in the crystalline phase of the pristine DNAA material at all temperatures.[54] This might be due to a higher dipolar response of DNAA inside the PHTP channel as compared with the pristine material. The increased dipole activity might generally result from an enhanced dipole density, ρ_μ, or an increased net dipole moment, μ, as predicted by eq 2. At a fixed temperature, T, for the DNAA/PHTP system, ρ_μ is constant. It is therefore highly probable that an enhanced μ of DNAA in PHTP channels lead to an increased ε'' intensity, in line with the amplification of the net dipole moment induced by the chain formation as predicted by the quantum-chemical calculations in Section 3.1.

Second, Figure 6 shows that the intensity of ε'' for the β_c process decreases gradually with increasing temperature, a feature often observed for macromolecules and associated with a crystallization process.[61−90] In DNAA/PHTP, this seems unlikely. Because of channel confinement, the loss of dielectric strength in Figure 8 might be explained by the net dipole vector, μ, of the inclusion compound and the resulting dipolar interaction factor, g. At elevated temperatures, small angle fluctuations due to dynamic distortions of the PHTP host lattice can induce substantial reduction in $\mu_{||}$ via the distortions from the collinear alignment, which lead to a decrease in ε. According to Figure 2a, a dipole reduction of 13% is expected even for small angles α, which is held responsible for the 21% reduction in the dielectric loss when going from 0 to 100 °C.

Further insight in the relaxation mechanism of the DNAA/PHTP system is obtained from its thermal activation. Unlike in zeolite L, the β_c process in Figure 7 is slower, occurring at about 128 °C higher (compared at 3 kHz), but in the temperature range of the pristine DNAA dynamics.[54] The β_c relaxation shows, generally, an Arrhenius-type thermal activation whose activation energy barrier gradually changes from 0.37 eV (∼ 36.3 kJ/mol) above 0 °C to 0.25 eV (∼ 24.5 kJ/mol) below 0 °C, interpreted as reduced intermolecular forces between channels.

In contrast to the pristine DNAA material, where antiparallel molecular stacks are formed, the channel architecture of PHTP imposes a quasi-1D environment: large interchannel distances (14−15 Å) and small channel diameters (4.5 Å) prohibit side-by-side stacking interactions as observed in pristine DNAA.[54] The one-dimensional molecular array in the channel can be visualized as a head-to-tail arrangement of molecules that are connected by flexible regions established by (weak) hydrogen bonds between the terminal polar nitro- and dimethylamino-groups;[33] the DNAA molecules themselves show a pronounced torsional flexibility in the azo region, which is easily thermally accessible as "wobbling mobility"; however, they are both derogated by the spatial confinement of the PHTP wall, as observed for related compounds by ^{2}H NMR and UV/vis experiments.[22] At low temperatures, this intramolecular mobility involving few rigid polar segments is faster with low activation energy (Figure 7), and its dielectric loss intensity is high (Figure 6) due to the dipole amplification. At elevated temperatures, the mobility involves many rigid polar segments, and thermal agitation further weakens the hydrogen bonding, leading to increased fluctuation angles α and, hence, to a reduction of the effective dipole moment. This is seen as a decrease in the dielectric loss intensity in Figure 6. With many segments involved, high activation energy is required, whereas the increased relaxation length scale slows down the process. Between the low and high temperature regions, the transitions from low to high activation energies as well as from fast to slow dynamics are gradual and lead to the unique changing Arrhenius-type thermal activation.

4. Concluding Remarks

A combination of complementary dielectric, spectroscopic, and microscopic techniques together with quantum-chemical calculations has been used to elucidate the alignment and molecular relaxation dynamics of a polar dye (DNAA) in two different nanochannel environments. Although zeolite L is rather hard but offers more spacious cavities, PHTP offers a tight but soft environment. In both zeolite L and PHTP channels, the

dye molecules align themselves in the general direction of the channel *c*-axis. In PHTP, a quasi-perfect one-dimensional collinear orientation of the dyes in the channels is observed, whereas molecules in zeolite L show significant deviation from collinearity and only partial filling of the channels and aggregation of chromophores at the channel entrances.

In contrast to the pristine DNAA material, in which intra- and intermolecular relaxations are detectable,[54] the molecular alignment due to channel confinement in zeolite L and PHTP imposes restrictions to the dynamics. In the less restrictive zeolite L cavity, *loosely* packed dyes (isolated molecules or dimeric units) can access high-amplitude rotational intramolecular (noncooperative) modes that exhibit Arrhenius-type behavior with an activation energy of 0.31 eV. Intermolecular modes are diminished because of the uncorrelated molecular distribution in the channels. In PHTP, rotational intramolecular modes are suppressed, and instead, intermolecular mobility is enhanced through dipole amplification and weak nitro−dimethylamino hydrogen bonds. The activation energy barrier of DNAA mobility in PHTP is temperature-dependent, as observed in other PHTP inclusion compounds;[22] they are reduced by 33% below 0 °C, which is attributed to diminishing intermolecular length scale of collective dynamics at low temperatures.

In view of the basic issues introduced at the beginning of this paper, charge transport (CT) along single PHTP channels is geometrically favored due to the close collinear arrangement. A recent theoretical study[91] has shown that transfer integrals in collinear arrangements can be optimized in short conjugated donor−acceptor-substituted systems due to the reduced delocalization of frontier orbitals. Although our present probe is not to be considered as the ideal guest to promote a high mobility for charge carriers, its packing in the organic channel is, however, in favor of it. At the same time, efficient photonic energy transfer (ET) was observed for PHTP inclusion compounds,[18,19] thus opening the way for novel materials for both efficient one-dimensional CT and ET. A drawback is the mechanical stability of PHTP host−guest systems, which suggests inorganic hosts as alternative materials. Although efficient ET was demonstrated for dye-loaded zeolite L systems,[19,92,93] we have demonstrated that CT will not be effective, since supramolecular wires, as in PHTP, cannot be created, essentially due to geometrical factors (cavity size) as well as specific host−guest interactions. Optimized materials to overcome these difficulties are sketchy and currently under investigation.

Acknowledgment. The authors thank the European Commission for financial support through the Human Potential Program (Marie-Curie RTN "Nanomatch" Contract No. MRTN-CT-2006-035884). J.G. is a "Ramón y Cajal" research fellow, financed by the Spanish Ministry for Science and Innovation. J.C. is an FNRS fellow. We thank H.-J. Egelhaaf (Nürnberg, Germany) for helpful discussions.

Supporting Information Available: Additional information as noted in text. This information is available free of charge via the Internet at http://pubs.acs.org.

References and Notes

(1) Oelkrug, D.; Tompert, A.; Gierschner, J.; Egelhaaf, H. J.; Hanack, M.; Hohloch, M.; Steinhuber, E. *J. Phys. Chem. B* **1998**, *102*, 1902.

(2) Oelkrug, D.; Egelhaaf, H. J.; Gierschner, J.; Tompert, A. *Synth. Met.* **1996**, *76*, 249.

(3) Pacios, R.; Chatten, A. J.; Kawano, K.; Durrant, J. R.; Bradley, D. D. C.; Nelson, J. *Adv. Funct. Mater.* **2006**, *16*, 2117.

(4) Luer, L.; Egelhaaf, H. J.; Oelkrug, D.; Cerullo, G.; Lanzani, G.; Huisman, B. H.; de Leeuw, D. *Org. Electron.* **2004**, *5*, 83.

(5) Calzaferri, G.; Gfeller, N. *J. Phys. Chem.* **1992**, *96*, 3428.

(6) Calzaferri, G.; Pauchard, M.; Maas, H.; Huber, S.; Khatyr, A.; Schaafsma, T. *J. Mater. Chem.* **2002**, *12*, 1.

(7) Megelski, S.; Lieb, A.; Pauchard, M.; Drechsler, A.; Glaus, S.; Debus, C.; Meixner, A. J.; Calzaferri, G. *J. Phys. Chem. B* **2001**, *105*, 25.

(8) König, O.; Bürgi, H.-B.; Armbruster, T.; Hulliger, J.; Weber, T. *J. Am. Chem. Soc.* **1997**, *119*, 10632.

(9) Botta, C.; Ferro, D. R.; Di Silvestro, G.; Tubino, R. *Structural and optical properties of conjugated molecules in perhydrotriphenylene (PHTP) and in other channel-forming inclusion compounds*, 1st ed.; Academic Press: San Diego/CA, 2001.

(10) Gierschner, K.; Luer, L.; Oelkrug, D.; Musluoglu, E.; Behnisch, B.; Hanack, M. *Adv. Mater.* **2000**, *12*, 757.

(11) Gierschner, J.; Luer, L.; Oelkrug, D.; Musluoglu, E.; Behnisch, B.; Hanack, M. *Synth. Met.* **2001**, *121*, 1695.

(12) Gierschner, J.; Egelhaaf, H. J.; Mack, H. G.; Oelkrug, D.; Alvarez, R. M.; Hanack, M. *Synth. Met.* **2003**, *137*, 1449.

(13) Botta, C.; Destri, S.; Pasini, M.; Picouet, P.; Bongiovanni, G.; Mura, A.; Uslenghi, M.; Di Silvestro, G.; Tubino, R. *Synth. Met.* **2003**, *139*, 791.

(14) Botta, C.; Bongiovanni, G.; Mura, A.; Di Silvestro, G.; Tubino, R. *Synth. Met.* **2001**, *116*, 175.

(15) Loi, M. A.; Mura, A.; Bongiovanni, G.; Botta, C.; Di Silvestro, G.; Tubino, R. *Synth. Met.* **2001**, *121*, 1299.

(16) Bongiovanni, G.; Botta, C.; Di Silvestro, G.; Loi, M. A.; Mura, A.; Tubino, R. *Chem. Phys. Lett.* **2001**, *345*, 386.

(17) Botta, C.; Treviganti, R.; Bongiovanni, G.; Mura, A.; Tubino, R. *Synth. Met.* **1999**, *101*, 565.

(18) Poulsen, L.; Jazdzyk, M.; Communal, J. E.; Sancho-Garcia, J. C.; Mura, A.; Bongiovanni, G.; Beljonne, D.; Cornil, J.; Hanack, M.; Egelhaaf, H. J.; Gierschner, J. *J. Am. Chem. Soc.* **2007**, *129*, 8585.

(19) Viani, L.; Tolbod, L.-P.; Jazdzyk, M.; Patrinoiu, G.; Cordella, F.; Mura, A.; Bongiovanni, G.; Botta, C.; Beljonne, D.; Cornil, J.; Hanack, M.; Egelhaaf, H.-J.; Gierschner, J. *J. Phys. Chem. B* **2009**, *113*, 10566.

(20) Gierschner, J.; Mack, H. G.; Luer, L.; Oelkrug, D. *J. Chem. Phys.* **2002**, *116*, 8596.

(21) Schilling, F. C.; Amundson, K. R.; Sozzani, P. *Macromolecules* **1994**, *27*, 6498.

(22) Srinivasan, G.; Villanueva-Garibay, J. A.; Muller, K.; Oelkrug, D.; Medina, B. M.; Beljonne, D.; Cornil, J.; Wykes, M.; Viani, L.; Gierschner, J.; Martinez-Alvarez, R.; Jazdzyk, M.; Hanack, M.; Egelhaaf, H. J. *Phys. Chem. Chem. Phys.* **2009**, *11*, 4996.

(23) Aloshyna, M.; Medina, B. M.; Poulsen, L.; Moreau, J.; Beljonne, D.; Cornil, J.; Di Silvestro, G.; Cerminara, M.; Meinardi, F.; Tubino, R.; Detert, H.; Schrader, S.; Egelhaaf, H. J.; Botta, C.; Gierschner, J. *Adv. Funct. Mater.* **2008**, *18*, 915.

(24) Vásquez, S. O. *Comput. Mater. Sci.* **2006**, *37*, 572.

(25) Zhang, N. R.; Mattice, W. L. *Acta Polym.* **1995**, *46*, 139.

(26) Tubino, R.; Fois, E.; Gamba, A.; Macchi, G.; Meinardi, F.; Minoia, A. *Stud. Surf. Sci. Catal.* **2005**, *155*, 501.

(27) Calzaferri, G.; Huber, S.; Maas, H.; Minkowski, C. *Angew. Chem., Int. Ed.* **2003**, *42*, 3732.

(28) Macchi, G.; Botta, C.; Calzaferri, G.; Catti, M.; Cornil, J.; Gierschner, J.; Meinardi, F.; Tubino, R. *Phys. Chem. Chem. Phys.* **2010**, *12*, 2599.

(29) Gervais, C.; Hertzsch, T.; Hulliger, A. *J. Phys. Chem. B* **2005**, *109*, 7961.

(30) Hulliger, J.; König, O.; Hoss, R. *Adv. Mater.* **1995**, *7*, 719.

(31) Megelski, S.; Calzaferri, G. *Adv. Funct. Mater.* **2001**, *11*, 277.

(32) Ruiz, A. Z.; Brühwiler, D.; Ban, T.; Calzaferri, G. *Monatsh. Chem.* **2005**, *136*, 77.

(33) Adams, H.; Allen, R. W. K.; Chin, J.; O'Sullivan, B.; Styring, P.; Sutton, L. R. *Acta Crystallogr., Sect. E: Struct. Rep. Online* **2004**, *60*, o289.

(34) Harley-Mason, J.; Mann, F. G. *J. Chem. Soc.* **1940**, 1379.

(35) Hulliger, J. *Angew. Chem., Int. Ed. Engl.* **1994**, *33*, 143.

(36) Wübbenhorst, M.; Klap, G. J.; Jansen, J. C.; van Bekkum, H.; van Turnhout, J. *J. Chem. Phys.* **1999**, *111*, 5637.

(37) Klap, G. J.; van Klooster, S. M.; Wübbenhorst, M.; Jansen, J. C.; van Bekkum, H.; van Turnhout, J. *J. Phys. Chem. B* **1998**, *102*, 9518.

(38) Huwe, A.; Kremer, F.; Karger, J.; Behrens, P.; Schwieger, W.; Ihlein, G.; Weiss, O.; Schuth, F. *J. Mol. Liq.* **2000**, *86*, 173.

(39) Huwe, A.; Kremer, F.; Behrens, P.; Schwieger, W. *Phys. Rev. Lett.* **1999**, *82*, 2338.

(40) Kremer, F.; Schoenhals, A. *Broadband Dielectric Spectroscopy*; Springer: Berlin, 2003.

(41) Havriliak, S.; Negami, S. *Polymer* **1967**, *8*, 161.

(42) Debye, P. J. W. *Polar Molecules*; Dover: New York, 1945.

(43) Böttcher, C. J. F.; Belle, O. C. V.; Bordewijk, P.; Rip, A. *Theory of Electric Polarization*, 2nd ed.; Elsevier Scientific Pub. Co.: Amsterdam, New York, 1973.

(44) Fröhlich, H. *Theory of Dielectrics Dielectric Constant and Dielectric Loss*, 2nd ed.; Clarendon Press: Oxford, 1958.

(45) Kirkwood, J. G. *J. Chem. Phys.* **1939**, *7*, 911.
(46) Onsager, L. *J. Am. Chem. Soc.* **1936**, *58*, 1486.
(47) Becke, A. D. *J. Chem. Phys.* **1993**, *98*, 1372.
(48) Frisch, M. J.; Trucks, G. W.; Schlegel, H. B.; Scuseria, G. E.; Robb, M. A.; Cheeseman, J. R.; Montgomery, J. A., Jr.; Vreven, T.; Kudin, K. N.; Burant, J. C.; Millam, J. M.; Iyengar, S. S.; Tomasi, J.; Barone, V.; Mennucci, B.; Cossi, M.; Scalmani, G.; Rega, N.; Petersson, G. A.; Nakatsuji, H.; Hada, M.; Ehara, M.; Toyota, K.; Fukuda, R.; Hasegawa, J.; Ishida, M.; Nakajima, T.; Honda, Y.; Kitao, O.; Nakai, H.; Klene, M.; Li, X.; Knox, J. E.; Hratchian, H. P.; Cross, J. B.; Bakken, V.; Adamo, C.; Jaramillo, J.; Gomperts, R.; Stratmann, R. E.; Yazyev, O.; Austin, A. J.; Cammi, R.; Pomelli, C.; Ochterski, J. W.; Ayala, P. Y.; Morokuma, K.; Voth, G. A.; Salvador, P.; Dannenberg, J. J.; Zakrzewski, V. G.; Dapprich, S.; Daniels, A. D.; Strain, M. C.; Farkas, O.; Malick, D. K.; Rabuck, A. D.; Raghavachari, K.; Foresman, J. B.; Ortiz, J. V.; Cui, Q.; Baboul, A. G.; Clifford, S.; Cioslowski, J.; Stefanov, B. B.; Liu, G.; Liashenko, A.; Piskorz, P.; Komaromi, I.; Martin, R. L.; Fox, D. J.; Keith, T.; Al-Laham, M. A.; Peng, C. Y.; Nanayakkara, A.; Challacombe, M.; Gill, P. M. W.; Johnson, B.; Chen, W.; Wong, M. W.; Gonzalez, C.; Pople, J. A. *Gaussian 03, Revision C.02*; Gaussian, Inc.: Wallingford CT, 2004.
(49) Moylan, C. R.; Twieg, R. J.; Lee, V. Y.; Swanson, S. A.; Betterton, K. M.; Miller, R. D. *J. Am. Chem. Soc.* **1993**, *115*, 12599.
(50) Yamamoto, S.; Nishimura, N.; Hasegawa, S. *Bull. Chem. Soc. Jpn.* **1971**, 44.
(51) van Walree, C. A.; Franssen, O.; Marsman, A. W.; Flipse, M. C.; Jenneskens, L. W. *J. Chem. Soc., Perkin Trans. 2* **1997**, 799.
(52) Datta, A.; Terenziani, F.; Painelli, A. *ChemPhysChem* **2006**, *7*, 2168.
(53) Cornil, D.; Olivier, Y.; Geskin, V.; Cornil, J. *Adv. Funct. Mater.* **2007**, *17*, 1143.
(54) Tsuwi, J.; Berger, R.; Behrnd, N.-R.; Ottiger, P.; Bertoni, M.; Prodi-Schwab, A.; Wübbenhorst, M.; Hulliger, A. submitted 2010 to *J. Phys. D: Appl. Phys.*
(55) Bossart, O.; De Cola, L.; Welter, S.; Calzaferri, G. *Chem.—Eur. J.* **2004**, *10*, 5771.
(56) Bossart, O. *Zeolite L Antenna Material for Organic Light Emitting Diodes and Organic Solar Cells*; Dissertation, University of Bern, 2006.
(57) Busby, M.; Blum, C.; Tibben, M.; Fibikar, S.; Calzaferri, G.; Subramaniam, V.; De Cola, L. *J. Am. Chem. Soc.* **2008**, *130*, 10970.
(58) Ramamurthy, V.; Sanderson, D. R.; Eaton, D. F. *J. Am. Chem. Soc.* **1993**, *115*, 10438.
(59) Del Cano, T.; Hashimoto, K.; Kageyama, H.; De Saja, J. A.; Aroca, R.; Ohmori, Y.; Shirota, Y. *Appl. Phys. Lett.* **2006**, 88.
(60) Bossart, O.; Calzaferri, G. *Chimia* **2006**, *60*, 179.
(61) Starkweather, H. W. *Macromolecules* **1981**, *14*, 1277.
(62) Bayer, A.; Hubner, J.; Kopitzke, J.; Oestreich, M.; Ruhle, W.; Wendorff, J. H. *J. Phys. Chem. B* **2001**, *105*, 4596.
(63) Wunderlich, B. *Prog. Colloid Polym. Sci.* **1994**, *96*, 22.
(64) Tomatsu, I.; Fitie, C. F. C.; Byelov, D.; de Jeu, W. H.; Magusin, P. C. M. M.; Wübbenhorst, M.; Sijbesma, R. P. *J. Phys. Chem. B* **2009**, *113*, 14158.
(65) Mierzwa, M.; Floudas, G.; Stepanek, P.; Wegner, G. *Phys. Rev. B* **2000**, *62*, 14012.
(66) Chen, Z. J.; Stepanenko, V.; Dehm, V.; Prins, P.; Siebbeles, L. D. A.; Seibt, J.; Marquetand, P.; Engel, V.; Wurthner, F. *Chem.—Eur. J.* **2007**, *13*, 436.
(67) Warman, J. M.; Van de Craats, A. M. *Mol. Cryst. Liq. Cryst.* **2003**, *396*, 41.
(68) Aliev, F. M.; Bengoechea, M. R.; Gao, C. Y.; Cochran, H. D.; Dai, S. *J. Non-Cryst. Solids* **2005**, *351*, 2690.
(69) Arrese-Igor, S.; Arbe, A.; Alegria, A.; Colmenero, J.; Frick, B. *J. Chem. Phys.* **2004**, *120*, 423.
(70) Arrese-Igor, S.; Arbe, A.; Colmenero, J.; Alegria, A.; Frick, B. *Phys. B: Condens. Matter* **2004**, *350*, 211.
(71) Bradshaw, M. J.; Raynes, E. P. *Mol. Cryst. Liq. Cryst.* **1981**, *72*, 73.
(72) Chandrasekhar, S.; Madhusudana, N. Y. *J. Phys. Colloq.* **1969**, *30*, 24.
(73) Drozd-Rzoska, A.; Rzoska, S.; Pawlus, S.; Ziolo, J. *Phys. Rev. E* **2005**, *72*, 031501.
(74) Elmahdy, M. M.; Floudas, G.; Mondeshki, M.; Spiess, H. W.; Dou, X.; Mullen, K. *Phys. Rev. Lett.* **2008**, *100*, 107801(1.
(75) Gennes, P. G. D. *The Physics of Liquid Crystals*; Clarendon Press: Oxford, 1975.
(76) Keil, D.; Hartmann, H.; Zug, I.; Schroeder, A. *J. Prakt. Chem. Chem./Ztg.* **2000**, *342*, 169.
(77) Kilian, D.; Knawby, D.; Athanassopoulou, M. A.; Trzaska, S. T.; Swager, T. M.; Wrobel, S.; Haase, W. *Liq. Cryst.* **2000**, *27*, 509.
(78) Labat, G.; Behrnd, N.-R.; Couderc, G.; Bonin, M.; Tsuwi, J.; Batagiannis, A.; Berger, R.; Bertoni, M.; Prodi-Schwab, A.; Hulliger, J. *Cryst. Eng. Commun.* **2010**, *12*, 1252.
(79) Longa, L.; Dejeu, W. H. *Phys. Rev. A* **1982**, *26*, 1632.
(80) Maier, W.; Saupe, A. *Z. Naturforsch., A: Astrophys. Phys. Phys. Chem.* **1960**, *15*, 287.
(81) Rai, P. K.; Denn, M. M.; Khusid, B. *Langmuir* **2006**, *22*, 2528.
(82) Riande, E.; Diaz-Calleja, R. *Electrical Properties of Polymers*; Marcel Dekker, Inc.: New York, 2004.
(83) Runt, J. P.; Fitzgerald, P. P. *Dielectric Spectroscopy of Polymeric Materials: Fundamentals and Applications*; ACS Books: Washington D.C., 1997.
(84) Thoen, J.; Menu, G. *Mol. Cryst. Liq. Cryst.* **1983**, *97*, 163.
(85) Tsuwi, J.; Hartmann, L.; Kremer, F.; Pospiech, D.; Jehnichen, D.; Häuβler, L. *Polymer* **2006**, *47*, 7189.
(86) Tsuwi, J.; Pospiech, D.; Jehnichen, D.; Häuβler, L.; Kremer, F. *J. Appl. Polym. Sci.* **2007**, *105*, 201.
(87) Urban, S.; Gestblom, B.; Dabrowski, R. *Phys. Chem. Chem. Phys.* **1999**, *1*, 4843.
(88) Van Roie, B.; Leys, J.; Denolf, K.; Glorieux, C.; Pitsi, G.; Thoen, J. *Phys. Rev. E* **2005**, *72*, 041702.
(89) Varadarajan, K.; Boyer, R. F. *J. Polym. Sci., Part B: Polym. Phys.* **1982**, *20*, 141.
(90) Yamamoto, S.; Nishimura, N.; Hasegawa, S. *Bull. Chem. Soc. Jpn.* **1971**, *44*, 2018.
(91) Viani, L.; Olivier, Y.; Athanasopoulos, S.; Demétrio, A.; Filho, D.; Hulliger, J.; Brédas, J.-L.; Gierschner, J.; Cornil, J. *ChemPhysChem* **2010**, *11*, 1062.
(92) Varun, V.; André, D.; Le-Quyenh, D.; Guido, S.; Marinella, C.; Gion, C.; Chiara, B. *Adv. Mater.* **2009**, *21*, 1146.
(93) Calzaferri, G. *Nuovo Cimento Soc. Ital. Fis., B* **2008**, *123*, 1337.

JP102451W